IEEE Access
Multidisciplinary | Rapid Review | Open Access Journal

Received December 16, 2019, accepted January 28, 2020, date of publication February 10, 2020, date of current version February 18, 2020.

Digital Object Identifier 10.1109/ACCESS.2020.2972568

Star Identification Algorithm Based on Image Normalization and Zernike Moments

XIAOBO LIANG[1,2], WENLI MA[1], JIN ZHOU[1], AND SIJIE KONG[1]
[1]Institute of Optics and Electronics, Chinese Academy of Sciences, Chengdu 610209, China
[2]College of Materials Science and Opto-Electronic Technology, University of Chinese Academy of Sciences, Beijing 100049, China

Corresponding author: Wenli Ma (mawenli@ioe.ac.cn)

This work was supported by the Institute of Optics and Electronics, Chinese Academy of Sciences.

ABSTRACT The star identification (star-ID) algorithm can match the stars captured by an optical system with a star catalog according to certain features. Star-ID has been an important research issue in many astronomical studies and a strong robust star-ID algorithm can effectively identify a certain number of stars as a standard source to correct uncalibrated telescopes. Generally, before star-ID, the celestial coordinates should be translated into the image coordinates with knowledge of optical center coordinates, image rotation angle, focal length of optical system, image sensor's pixel size and so on. For an uncalibrated telescope, the star-ID performance usually suffers from the errors or even the lack of these parameters. In this paper, a novel star-ID algorithm is devised which is based on image normalization technique and the Zernike moment such that the invariant features of asterisms are extracted instead of traditional ways. And three real images which captured via an uncalibrated ground-based telescope are used to validate our method, and the results show that it can effectively identify stars with a success rate of 99.27%, which demonstrate the robustness and accuracy of the proposed method.

INDEX TERMS Image normalization, star identification, Zernike moment.

I. INTRODUCTION

The star-ID algorithm is a basic algorithm in the astronomical research which has a wide application in many fields such as navigation, attitude determination and error correction. Its essence is to compare certain features to those in a catalog. To determine the transforming relationship between the celestial coordinates of the catalog and the pixel coordinates of the star point, many parameters are required, such as optical center pixel coordinates, image rotation angle, optical system focal length, pixel size of image sensor, pointing of telescope and so on. These parameter errors listed in Table 1 have different effects on the final coordinate conversion result.

For an uncalibrated telescope, the initial parameters often contain large errors which will affect the results of coordinate transformation and feature extraction, and ultimately cause a negative impact on star-ID.

The key to solving this problem is to find proper invariant features independent of the equipment's parameters. At present, many approaches have been adopted to improve the performance of the extracted features. In 1995, Liebe used two angular distances and a spherical angle between the two neighbouring stars as a feature to identify stars [1]. This method can solve the identification problem under translation and rotation transformation, but a pattern of three stars is too simple to ensure success rate when identify the faint stars. In 1996, Quine and Durrant-Whyte proposed an algorithm which is similar to that of Liebe and a scale-invariant feature is added [2]. In 1997, Padgett and Kreutz-Delgado proposed the grid algorithm which can extract translation and rotation invariant features [3]. However, the main defect of grid algorithm is that its recognition depends on the correct selection of the nearest neighboring star and cannot directly identify neighboring stars. In 2008, Yang *et al.* improved the grid algorithm which can extract scale-invariant features by using the distance between nearest neighboring star and the reference star as a standard scale factor [4]. By using this method, the recognition problem under translation, rotation and scale transformation is solved. In 2008, Zhang *et al.* used radial and cyclic star pattern to identify stars, this method does not depend on the selection result of the nearest neighboring star to calculate the image rotation [5]. In 2013, Ji *et al.* improved the radial and cyclic star pattern, acquiring a translation, rotation and scale invariant feature [6], but it is sensitive to

The associate editor coordinating the review of this manuscript and approving it for publication was Changsheng Li.

TABLE 1. The impacts of parameters on coordinate transformation.

Parameter name	Impact on Transformation Results	Linear/Nonlinea
optical center pixel coordinates (X_0, Y_0)	translation transformation	linear
image rotation angle (α)	rotation transformation	linear
focal length (f)	scaling transformation	linear
CCD pixel size (p_x, p_y)	scaling transformation	linear
CCD vertical error	skew transformation	linear
pointing of telescope (A,E)	nonlinear error	nonlinear
optical system distortion	nonlinear error	nonlinear

the number and magnitude of stars. In 2015, Aghaei and Moghaddam developed an iterative algorithm to eliminate the spurious candidate stars and find the true match [7]. In 2016, Ji *et al.* proposed a parameter estimation method to optimize the grid algorithm [8]. In 2019, Win *et al.* used the dynamic cyclic features to suppress the star group's position noise and magnitude noise [9].

Although the above researches have shown considerable success in star-ID, however, they can only partially meet the requirements under our situation. To solve this problem thoroughly, an extreme case is assumed where the first four parameters in Table 1 are completely missing, at the same time, there is an error in the telescope pointing, the image sensor is tilted, and the optical system distortion is unsolved. Our invariant feature extraction method is realized by implementing image normalization technique and Zernike moments to eliminate the negative influence outlined above.

The performance of our algorithm is tested by using three images acquired by the telescope whose aperture is 600 mm. In this process, we totally identify 216 reference stars and 864 neighboring stars. Meanwhile, we compared the proposed method with Yang *et al.*'s [4], Li *et al.*'s [6], Ji *et al.*'s [8], and Win *et al.*'s [9] algorithms. Note that the radial feature is not a scale invariant feature. To test this algorithm under the same conditions, a method similar to reference 4 is used to extract scale invariant features.

The results show that the algorithm of this paper correctly identifies 137 star groups in three star images with 99.27% success rate. While Yang *et al.*'s algorithm identifies 119 star groups with accuracy of 94.96%, Ji *et al.*'s algorithm identifies 129 star groups with accuracy of 96.12%, Mahdi et al.'s algorithm identifies 113 star groups with accuracy of 99.12%, and Xin et al.'s algorithm identifies 122 star groups with accuracy of 97.54%. But, when the star image is mirrored or severely tilted, the four comparative algorithms are completely invalid while the algorithm in this paper is not affected by the two factors. The results show that our algorithm offers conspicuous advantages over existing star-ID algorithms under the condition of some specific parameters of our telescope lacking with better robustness and accuracy.

The chapters of this article are arranged as follows. Chapter 2 gives the proof of affine transformation relationship. Chapter 3 describes the star image normalization. Chapter 4 discusses the way of Zernike moments calculation. Chapter 5 introduces the method of star choosing and identification. Chapter 6 analyzes the result of our experiment. Chapter 7 concludes this paper with a discussion.

II. PROOF OF THE AFFINE RELATIONSHIP

Affine transformation is a kind of linear transformation including translation, rotation, scaling and skew. It is the mathematical basis of image normalization, so in this paper, we first give the proof that the star's pixel coordinates calculated by inaccurate parameters in Table 1 are actually an affine transformation of the coordinates under the ideal parameters. To simplify the proof process, only one star's affine transformation relationship is given. The proof for multiple stars is similar with this.

A. TRANSFORMATION FROM CELESTIAL COORDINATES TO PIXEL COORDINATES

The transformation from celestial coordinates to pixel coordinates is a nonlinear process. We have given this coordinate transformation method in our previous work [10]. It is note worth that the parameter errors in Table 1 do not affect the calculation of theoretical azimuth and elevation angle (AE) of the star, so only the conversion algorithm from angle coordinates to pixel coordinates is given here, and this is a linear process as can be seen from formula 1 to 9.

Let P and $R_{(\alpha)}$ denote the scaling matrix and the rotation matrix, respectively.

$$P = \begin{bmatrix} \frac{1}{p_x} & 0 \\ 0 & -\frac{1}{p_y} \end{bmatrix}, \tag{1}$$

$$R_{(\alpha)} = \begin{bmatrix} \cos\alpha & -\sin\alpha \\ \sin\alpha & \cos\alpha \end{bmatrix}. \tag{2}$$

Here p_x and p_y represent the pixel size of CCD in the x and y directions, respectively. α is the rotation angle of the star image.

Then, the transformation from angle coordinates to pixel coordinates can be expressed by a liner equation:

$$\begin{bmatrix} X \\ Y \end{bmatrix} = P \cdot R_{(\alpha)} \begin{bmatrix} x \\ y \end{bmatrix} + \begin{bmatrix} X_0 \\ Y_0 \end{bmatrix}. \tag{3}$$

where $(X, Y)^T$ represents the pixel coordinates of a star, $(x, y)^T$ is the distance from optical center in millimeter which

can be calculated from formula 4 [11].

$$\begin{cases} x = \tan \Delta A \cdot (f \cos E_0 - y \sin E_0) \\ y = f \cdot \dfrac{\tan E \cdot \cos E_0 - \cos \Delta A \cdot \sin E_0}{\tan E \cdot \sin E_0 + \cos \Delta A \cdot \cos E_0} \\ \Delta A = A - A_0. \end{cases} \tag{4}$$

In formula 4, f represents the focal length of the telescope optical system; $(A, E)^T$ represents the AE of the star; $(A_0, E_0)^T$ represents AE of the optical center.

B. PROOF OF THE AFFINE RELATIONSHIP

Assuming that some of the parameters in Table 1 contain the errors which shown in formula 5.

$$\begin{cases} f' = a \cdot f \\ p'_x = b_1 \cdot p_x \\ p'_y = b_2 \cdot p_y \\ X'_0 = X_0 + \Delta X_0 \\ Y'_0 = Y_0 + \Delta Y_0 \\ \alpha' = \alpha + \Delta\alpha. \end{cases} \tag{5}$$

Suppose that there is no error in $(A, E)^T$ and $(A_0, E_0)^T$. Mathematically, the star pixel coordinates calculated with the parameter error can be represented in formula 6:

$$\begin{aligned} \begin{bmatrix} X' \\ Y' \end{bmatrix} &= P' \cdot R_{(\alpha')} \begin{bmatrix} x' \\ y' \end{bmatrix} + \begin{bmatrix} X'_0 \\ Y'_0 \end{bmatrix} \\ &= a \begin{bmatrix} \frac{1}{b_1} & 0 \\ 0 & \frac{1}{b_2} \end{bmatrix} \cdot P \cdot R_{(\Delta\alpha)} \cdot P^{-1} \begin{bmatrix} X - \Delta X_0 \\ Y - \Delta Y_0 \end{bmatrix} \\ &\quad + \begin{bmatrix} X_0 + \Delta X_0 \\ Y_0 + \Delta Y_0 \end{bmatrix} \end{aligned} \tag{6}$$

Define A and B as:

$$A = a \begin{bmatrix} \frac{1}{b_1} & 0 \\ 0 & \frac{1}{b_2} \end{bmatrix} \cdot P \cdot R_{(\Delta\alpha)} \cdot P^{-1} = \begin{bmatrix} a_{11} & a_{12} \\ a_{21} & a_{22} \end{bmatrix}, \tag{7}$$

$$B = \begin{bmatrix} X_0 + \Delta X_0 \\ Y_0 + \Delta Y_0 \end{bmatrix} - A \begin{bmatrix} X_0 \\ Y_0 \end{bmatrix} = \begin{bmatrix} b_{11} \\ b_{12} \end{bmatrix}. \tag{8}$$

Then the formula 6 can be written as the following form:

$$\begin{bmatrix} X' \\ Y' \end{bmatrix} = A \begin{bmatrix} X \\ Y \end{bmatrix} + B, \tag{9}$$

where A is a 2-by-2 constant coefficients matrix and B is a 2-by-1 constant coefficients matrix.

The formula 9 shows that there is a strict affine transformation relationship between the errorless pixel coordinates and the error containing pixel coordinates.

III. STAR IMAGE NORMALIZATION

Having proved that the calculation error of pixel coordinates of star caused by parameter errors is essentially equivalent to an affine transformation of error-free coordinates. The normalization technique of image can effectively eliminate the transformation factor generated by an affine transformation, and gets a ''standard'' image. Theoretically, the ''standard'' images of arbitrary affine transformed images are strictly consistent [12], and can be used to extract invariant features when the parameters are missing [13], [14].

There are at least two advantages to applying normalization to star identification. First, by calculating the pixel coordinates of the star's center [15], the image can be transformed into a sparse matrix, which can effectively reduce the amount of computation and improve the efficiency of the algorithm. Second, the index of a digital image is integral, however, our ultimate goal is to extract features from original image rather than restore the star image. We extract features directly from non-integer star pixel coordinates to effectively avoid redigitization errors.

First, let $(X_s, Y_s)^T$ denote the center of the star spot extracted from the star image. Then, re-denote the image signature by $p_{(X_s,Y_s)}$ in formula 10.

$$p_{(X_s,Y_s)} = \begin{cases} 1 : star\ center \\ 0 : background, \end{cases} \tag{10}$$

And finally, a star image is turned into a sparse binary matrix. This matrix is independent of magnitude, which can effectively reduce the interference of magnitude uncertainty to the feature extraction, and also effectively reduce the time and space complexity of the algorithm.

Then, formula 11 can be employed to calculate the origin moment of a star group.

$$m_{ij} = \sum_{X_s} \sum_{Y_s} X_s^i Y_s^j \, p_{(X_s,Y_s)}. \tag{11}$$

And the center of the group can be denoted as follows:

$$\begin{cases} \bar{X}_s = m_{10}/m_{00} \\ \bar{Y}_s = m_{01}/m_{00}. \end{cases} \tag{12}$$

Let formula 13 denote the central moments of $i + j$ order:

$$\bar{m}_{ij} = \sum_{X_s} \sum_{Y_s} (X_s^i - \bar{X}_s)^i (Y_s^j - \bar{Y}_s)^j \, p_{(X_s,Y_s)}. \tag{13}$$

And, then define M as:

$$M = \begin{bmatrix} \bar{m}_{20} & \bar{m}_{11} \\ \bar{m}_{11} & \bar{m}_{02} \end{bmatrix}. \tag{14}$$

Let λ_1 and λ_2 denote two eigenvalues of $M(\lambda_1 \geq \lambda_2)$, and $e_1 = [e_{1x}, e_{1y}]^T$ and $e_2 = [e_{2x}, e_{2y}]^T$ represents the two corresponding unit eigenvectors. It has the property: $e_1 \cdot e_2 = 0$.

Define rotation matrix as:

$$E = \begin{bmatrix} e_{1x} & e_{1y} \\ -e_{1y} & e_{1x} \end{bmatrix}, \tag{15}$$

scale matrix as:

$$W = \mathrm{diag}\left(\frac{c}{\sqrt{\lambda_1}}, \frac{c}{\sqrt{\lambda_2}}\right), \quad c = (\lambda_1 \lambda_2)^{\frac{1}{4}}. \tag{16}$$

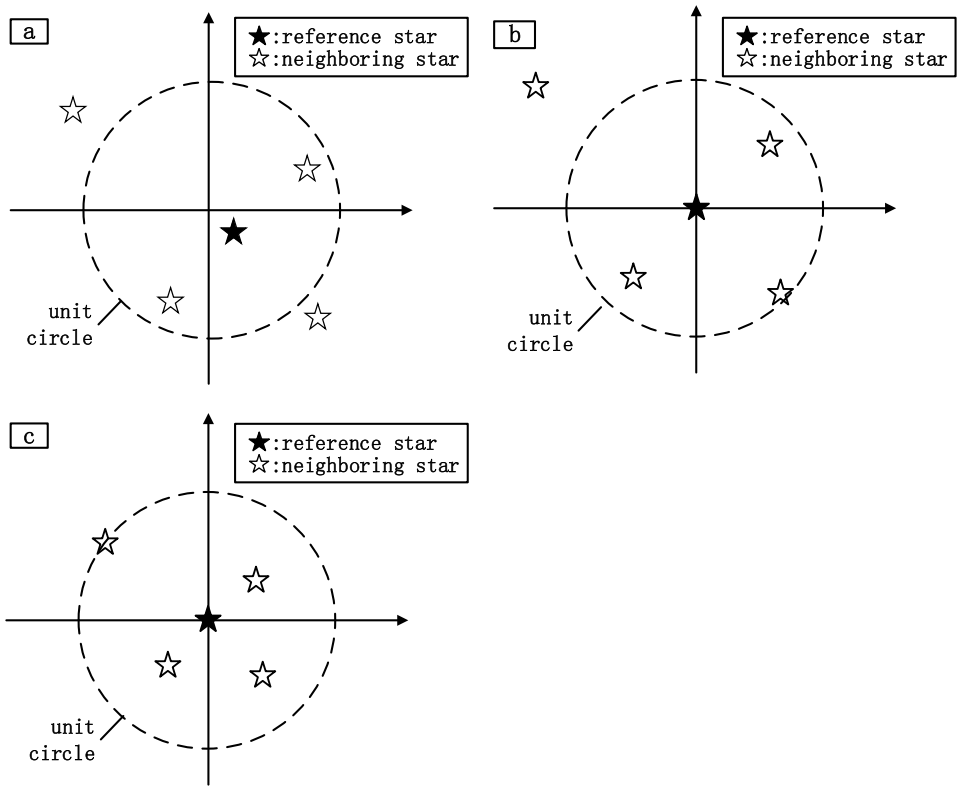

FIGURE 1. Unit circle mapping diagram. (a) Normalized star group, (b) star group translation, (c) star group mapping to unit circle.

At last, the normalization of the image can be denoted as:

$$\begin{bmatrix} X_s' \\ Y_s' \end{bmatrix} = WE \begin{bmatrix} X_s - \bar{X}_s \\ Y_s - \bar{Y}_s \end{bmatrix}. \tag{17}$$

where $(X_s', Y_s')^T$ denotes the normalized star position corresponding to $(X_s, Y_s)^T$.

IV. ZERNIKE MOMENTS CALCULATION

Zernike moments have extensive applications in image reconstruction [16], target recognition [17], feature detection [18] and so on. Using Zernike moments as a feature has many advantages. In this paper, we mainly utilize its rotation invariance, mirror invariance, and fast calculation properties. Note that Zernike moment is not a scale invariant feature [19], so the star group is pre-processed by the star image normalization. Star image after normalization is actually a set of discrete points. Using Zernike moments as a feature has three advantages: (1) Using the appropriate number of moments as features can effectively improve the success rate of the star-ID algorithm; (2) the features extracted by Zernike moment are mirror-independent; (3) star-ID can be accomplished without cyclic shift.

A. UNIT CIRCLE MAPPING

Zernike moment is a complex number defined in the unit circle. Before calculating the moment, the coordinates of the star center must be mapped to the unit circle. Fig. 1 shows this mapping process. First, translate all star points according to the reference star coordinate, so that the reference star is located at the origin of the coordinate, as shown in Fig. 1 (a) and Fig. 1 (b); second, find the neighboring star that is farthest from the reference star and calculate the corresponding distance d_{max}; finally, use d_{max} as the scale factor to perform rotation-free scale transformation on the star point coordinates, as shown in Fig. 1 (c).

B. ZERNIKE MOMENTS CALCULATION

After mapping the star group to the unit circle, the corresponding Zernike moments of $n + m$ order can be calculated according to the formulas 18 to 20 [16]:

$$Z_{\mathrm{nm}}(x, y) = \frac{n+1}{\pi} \sum_x \sum_y V_{nm}^*(x, y) p(x, y), \tag{18}$$

$$V_{\mathrm{nm}}(x, y) = R_{\mathrm{nm}}(x, y) \exp(jm \tan^{-1} \frac{y}{x}), \tag{19}$$

and

$$R_{\mathrm{nm}}(x, y) = \sum_{s=0}^{(n-|m|)/2} (-1)^s \frac{(n-s)!}{s!(\frac{n+|m|}{2}-s)!(\frac{n-|m|}{2}-s)!} \times (\sqrt{x^2+y^2})^{(n-2s)}, \tag{20}$$

where n and m satisfy constraint conditions $\mathrm{mod}(n-m, 2) = 0$ and $0 \le m \le n$.

Noting that Z_{nm} is a complex number, we take the $|Z_{nm}|$ as a feature to accomplish the final identification.

The feature extraction method of this paper is independent of magnitude information considering the features may be contaminated by the large star magnitude noise (usually $\pm 0.2 \sim 0.3$ magnitudes).

Up to now, the feature extraction method of star group is compendiously described which can minimize the reliance on the parameters in Table 1. It is noteworthy that the features extracted by this method are also invariant to tilt or mirror transformation.

V. STAR CHOOSING AND IDENTIFICATION

A. STAR CHOOSING IN IMAGE

The bright star in the image usually has larger centroiding error, which is not suitable as a high-precision standard source. So, this paper identifies the stars with less polluted and relatively faint.

The number of faint stars is more than bright ones, to distinguish each pattern from massive other stars in the catalog, we employ a star group consisting of one reference star and four neighboring stars to raise the probability of unique star-ID results.

The selection method is as follows:

(1) Select a relatively faint star that can calculate high-precision centroid coordinates as the reference star; (2) take the reference star as the center, all the neighboring stars which can accurately calculate the centroid coordinates are found within a small neighborhood (the radius of the neighborhood is 70 pixels in this paper); (3) calculate the magnitude of the searched out neighbouring stars; (4) sort and select top 4 neighbouring stars with the highest brightness to form the five-star mode. And the reference star with insufficient neighbouring stars will be ignored.

There are three advantages to adopt this strategy:

(1) it can effectively avoid selecting stars that are not recorded in the catalogue; (2) it is conducive to subsequent screening and reducing the number of the stars in catalogue; (3) it is beneficial to lower the mismatching rate, increase success rate and improve the efficiency of the algorithm.

B. STAR CHOOSING IN CATALOG

In this paper, we use the Fourth U.S. Naval Observatory CCD Astrograph Catalog (UCAC4) as the main catalog, and filter it according to the pointing and field of view (FOV) of our telescope.

The selection method is as follows:

(1) Select reference star candidates according to the magnitude calculated from the image and magnitude error;
(2) select top $N(N > 4$, and $N = 15$ in this paper) stars with the highest brightness near each candidate reference star.

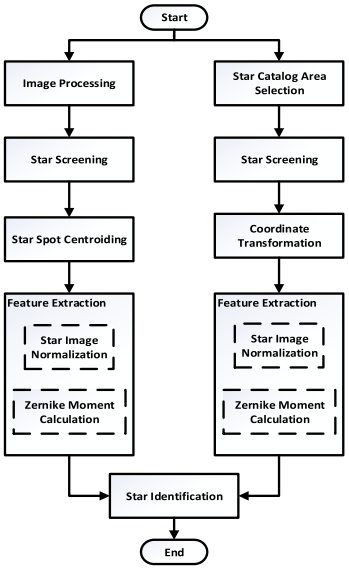

FIGURE 2. Algorithm flowchart.

C. STAR IDENTIFICATION

We apply multiple Zernike moments as features to reduce the ambiguities of star pattern. For a star group, SG, in an image, supposes that its pattern formed by multiple Zernike moments extracted from SG is shown in formula 21.

$$\mathrm{pat}_{\mathrm{nm}}^{im}(SG) = (\left|Z_{00}^{im}\right|, \left|Z_{02}^{im}\right|, \ldots, \left|Z_{0m}^{im}\right|, \ldots, \left|Z_{nm}^{im}\right|). \quad (21)$$

And, assuming that Q star groups are totally selected from the catalog according to the method in chapter 5.B. For each reference star, there are C_N^4 kinds of combinations of neighboring stars.

After the coordinate transformation, the Zernike moments of the star group are calculated, let $\mathrm{pat}_{\mathrm{nm}}^{\mathrm{cat}}(SG_{\mathrm{i}}^{\mathrm{j}})$ denote the pattern of the star group consisting of the ith reference star and the combination of its jth neighboring stars. And, its expression is shown in formula 22.

$$\mathrm{pat}_{\mathrm{nm}}^{\mathrm{cat}}(SG_{\mathrm{i}}^{\mathrm{j}}) = (\left|Z_{00}^{im}\right|, \left|Z_{02}^{im}\right|, \ldots, \left|Z_{0m}^{im}\right|, \ldots, \left|Z_{nm}^{im}\right|),$$
$$i = 1, 2, \ldots, Q. \quad \mathrm{j} = 1,2,\ldots,\mathrm{C}_N^4. \quad (22)$$

Using formula 23 to measure the similarity between SG and $SG_{\mathrm{i}}^{\mathrm{j}}$. Then, the $SG_{\mathrm{i}}^{\mathrm{j}}$ who satisfy formula 24 are considered as the identified stars.

$$J_{\mathrm{nm}}(pat_{nm}^{im}, pat_{nm}^{cat}) = \sum_{k=0}^{n}\sum_{l=0}^{m} \frac{\left|\left|Z_{kl}^{im}\right| - \left|Z_{kl}^{cat}\right|\right|}{\left|Z_{kl}^{cat}\right|}, \quad (23)$$

where $\mathrm{mod}(n-m, 2) = 0, 0 \le m \le n$.

$$\arg\min(J_{nm}) \quad \text{and} \quad \min(J_{nm}) < \varepsilon, \quad (24)$$

where ε is a threshold to prevent false alarms.

The flow chart of our algorithm is shown in Fig. 2.

The image processing module is used to find all objects within a certain magnitude range; the star catalog area selection module is mainly used to reduce the number of stars

TABLE 2. Comparison of the prior value and the input.

Parameter name	Prior value of image #1	Prior value of image #2	Prior value of image #3	Input 1	Input 2	Unit
optical center pixel coordinates (X_0, Y_0)	[1014,1005]	[1014,1005]	[1014,1005]	[0,0]	[0,0]	pixel
image rotation angle (α)	-1.5731768	-0.5540649	-0.5753618	0.0	0.0	rad
focal length (f)	830.0	830.0	830.0	1.0	1.0	mm
CCD pixel size (p_x, p_y)	[0.024,0.024]	[0.024,0.024]	[0.024,0.024]	[0.01,0.01]	[0.01,0.02]	mm/pixel
is image mirrored?	No	No	No	No	Yes	
is pointing calibrated?	No	No	No	No	No	
is distortion of optical system corrected?	No	No	No	No	No	

to be matched according to the pointing and FOV; star spot centroiding can locate the star's peak to sub-pixel precision; coordinate transformation is used to convert the celestial reference coordinates of a star under the catalog's epoch to the pixel coordinate under the current epoch; the feature extraction module has been discussed in detail in chapter 3 and chapter 4; star identification is used to find the optimal matching results according to the invariant features.

The pixel position of stars formed on CCD through the optical system of telescopes can be calculated accurately according to the telescope location, telescope pointing, distortion coefficient, optical system parameters, CCD parameters, etc. Ideally, the Zernike feature vector calculated by the catalog through coordinate transformation is invariant to the feature that directly calculated by the pixel coordinates of the same star group. However, these parameters will have some errors in practice, and have a negative impact on feature extraction. We divide the factors that affect the results of coordinate transformation into two categories. One is composed of optical system parameters and CCD parameters, its adverse effects can be eliminated by image normalization, and the corresponding proofs have been given in chapter 2.B; the other consists of the telescope location, pointing and distortion coefficient, etc. Considering the background of this paper, it is difficult to completely eliminate errors caused by such factors. To suppress these errors, the methods in chapter 5 are used to select reference stars and neighbouring stars. By selecting several neighboring stars in a small neighborhood near the reference star, this kind of error can be suppressed by means of coordinate translation, because the error caused by pointing error and distortion can be considered as a constant in a small neighborhood. In addition, formula 23 is used to evaluate the similarity of star group's features in the catalog and image, and threshold ε is employed to describe the tolerance of this error. The robustness of our algorithm will be tested without correcting the telescope pointing and distortion, and the corresponding results will be analyzed in chapter 6.

VI. EXPERIMENTS AND RESULTS

Taking advantage of the feature extraction method outlined in chapters 3 and 4, the novel star-ID algorithm is employed to process three real sky images. Our experiment is used to identify the recognize performance from real image by using a ground-based telescope. The diameter of our telescope is 600mm with a focal distance of 830mm. In addition, it employs a single 16-bit (2040 × 2040) chips, with a reference pixel-scale of $5.94''/pix$ (0.024mm/pix), providing a total FOV of $\sim 3.37^\circ \times 3.37^\circ$. And, the algorithm was implemented using C++ language, on a PC (CPU: Intel Core i5-3210M 2.5 GHz, RAM: 8 GB).

Table 2 shows the partial prior values of parameters in Table 1. To verify the performance of our algorithm under the parameters missing conditions, a set of arbitrary values is chosen as the input. Meanwhile, the robustness of our algorithm is tested by identify stars without correcting telescope pointing and distortion.

We totally identify 216 star groups (71 star groups in image #1, 71 star groups in image #2, and 74 star groups in image #3) in Fig. 3 in which the reference stars are red pentacled while the neighboring stars are green circled. To test the robustness of the algorithm, we do not eliminate the star group which contains double star, large proper motion star and star not recorded in the UCAC4. We respectively use the proposed algorithm, an improved grid algorithm [4], an improved radial and cyclic star pattern [6], a grid algorithm using optimization approaches [8], and a radial and dynamic cyclic star pattern to identify stars [9], and their final results are compared.

Testing based on the prior value is performed to evaluate the identification ability under normal conditions. And input 1 is used to verify the identification ability of the five algorithms in the absence of four major coordinate transformation parameters. While the input 2 is to further test the performance when the image is mirrored and the image sensor is tilted.

Before star-ID, the number of Zernike moments which we used in this paper must be decided. A star group has an infinite number of Zernike moments. However, in practice, a limited number of moments are used for star-ID. In this paper, the performance of the algorithm under different numbers of Zernike moments is tested by the star image #1 and the corresponding results are compared under the condition of input 2 in Table 2 and the corresponding results are shown in Table 3.

Table 3 shows that when identification threshold is stationary, the accuracy of star-ID decreases with the use of a small number of Zernike moments, while when a large number

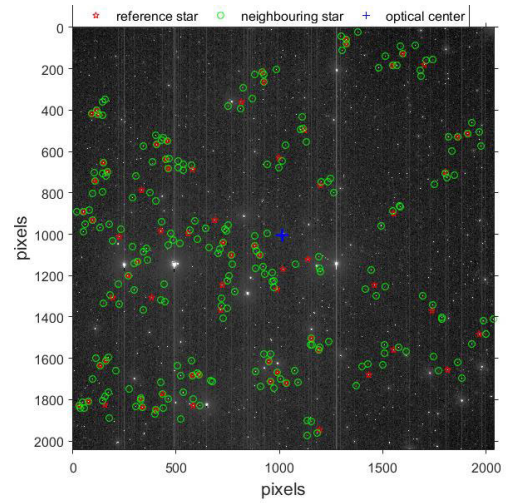

(a) Star image #1

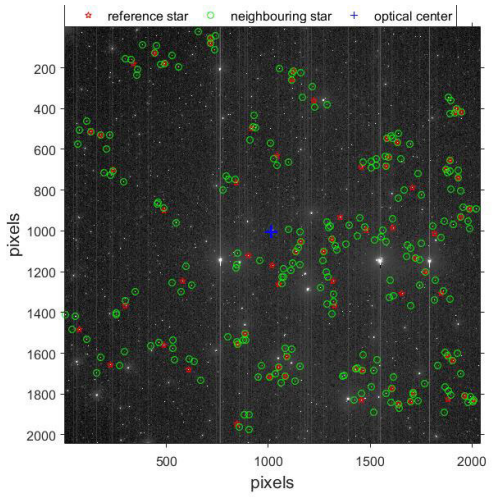

(b) Mirrored star image #1

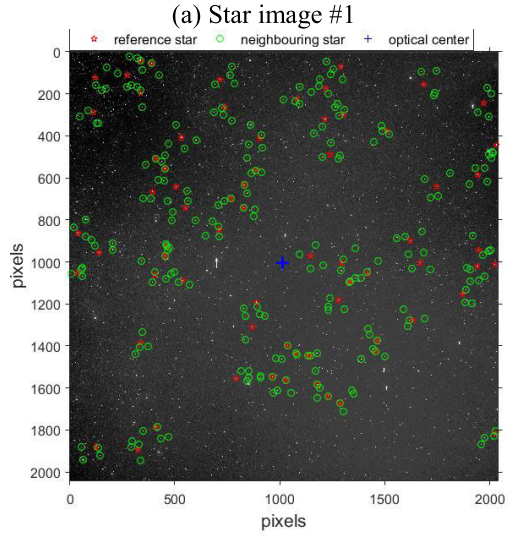

(c) Star image #2

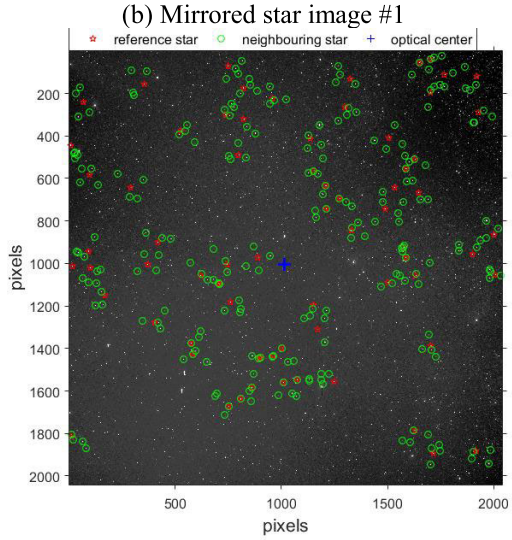

(d) Mirrored star image #2

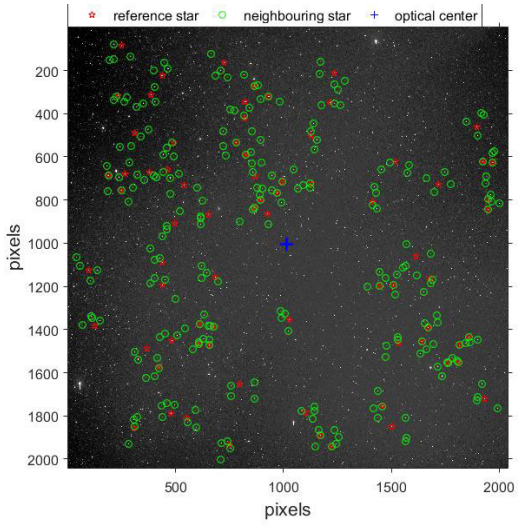

(e) Star image #3

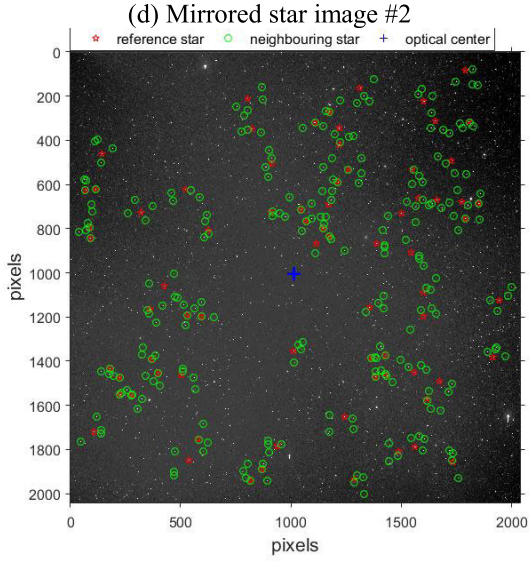

(f) Mirrored star image #3

FIGURE 3. The three images used in this paper. The coordinates of the center of the field of the image #1 are RA = 02h06m18s, DEC = 26°08′34″ (J2000.0). The coordinates of the center of the field of the image #2 are RA = 19h02m47s, DEC = 07°51′02″ (J2000.0). The coordinates of the center of the field of the image #3 are RA = 17h48m55s, DEC = −04°10′27″ (J2000.0).

TABLE 3. Algorithm performance under different number of Zernike moments ($\varepsilon = 0.6$).

(n,m)	Number of Zernike moments	Number of identified star groups	Number of correctly identified star groups	Success rate	Running time
(4,4)	9	71	61	85.92%	400.68s
(6,6)	16	64	59	92.19%	625.12s
(8,8)	25	61	58	95.08%	962.88s
(10,10)	36	54	54	100%	1466.73s
(12,12)	49	46	46	100%	2095.49s
(14,14)	64	46	46	100%	3210.13s

TABLE 4. Identification Results of image #1.

	Number of identified reference stars			Number of identified neighbouring stars			Success rate		
	Prior value	Input 1	Input 2	Prior value	Input 1	Input 2	Prior value	Input 1	Input 2
Our method	54	54	54	216	216	216	100%	100%	100%
Comparative method 1 [4]	51	51	2				92.16%	92.16%	0%
Comparative method 3 [6]	51	50	7	204	200	28	96.08%	98.00%	0%
Comparative method 2 [8]	44	44	0				100%	100%	0%
Comparative method 4 [9]	46	47	6	184	188	24	97.83%	97.87%	0%

TABLE 5. Identification Results of image #2.

	Number of identified reference stars			Number of identified neighbouring stars			Success rate		
	Prior value	Input 1	Input 2	Prior value	Input 1	Input 2	Prior value	Input 1	Input 2
Our method	42	42	42	168	168	168	100%	100%	100%
Comparative method 1 [4]	32	32	9				96.88%	96.88%	0%
Comparative method 3 [6]	35	35	6	140	140	24	97.14%	97.14%	0%
Comparative method 2 [8]	34	34	0				97.06%	97.06%	0%
Comparative method 4 [9]	34	35	6	136	140	24	97.06%	97.14%	0%

TABLE 6. Identification results of image #3.

	Number of identified reference stars			Number of identified neighbouring stars			Success rate		
	Prior value	Input 1	Input 2	Prior value	Input 1	Input 2	Prior value	Input 1	Input 2
Our method	41	41	41	164	164	164	97.56%	97.56%	97.56%
Comparative method 1 [4]	36	36	8				97.22%	97.22%	0%
Comparative method 3 [6]	43	43	2	172	172	8	95.35%	95.35%	0%
Comparative method 2 [8]	35	35	0				100%	100%	0%
Comparative method 4 [9]	42	39	3	168	156	12	97.62%	97.44%	0%

of Zernike moments are used, the number of identified star groups will be significantly reduced, and the running time of the algorithm will be significantly increased.

Therefore, in this paper, 36 different Zernike moments are used as features in our experiment. And to ensure the reliability of the star-ID results, a conservative identification threshold ($\varepsilon = 0.6$) is applied to lower the false alarm rate, although this will increase the missing alarm rate.

We use the same parameters to identify the star groups in the other two star images, and the identification results under the corresponding prior values, input 1 and input 2 are respectively shown in Table 4 to 6.

From Table 4 to 6, we can draw the conclusion that under the prior value and input 1, all the five algorithms can identify star groups effectively, but our algorithm has a better accuracy and recognition rate. And none of the four comparative algorithms can effectively identify the stars under input 2, and even some algorithms get wrong identification results. Note that the features extracted by the grid algorithm and the radial and cyclic feature algorithm are not independent to the mirror and tilt transformation, thus impose a negative affects to the identification results, therefore, none of the four comparative algorithms can identify star groups effectively when the image is mirrored and the image sensor is tilted, while our algorithm guarantees the success rate for mirrored image.

When using our star-ID algorithm to identify the star groups in Fig. 3 (a) and (b), 17 star groups are not successfully identified among which 8 missed alarm for the small ε, 7 are interfered by binary stars or bad pixels, and 2 contained star which are not in the UCAC4 catalog. And 29 star groups are failed to identify when using Fig. 3 (c) and (d) as input image, among them 17 missed alarm for the small ε, 10 are interfered by binary stars or bad pixels, and 2 contained star which are not in the UCAC4 catalog. Furthermore, Fig. 3 (e) and (f) contain 33 unrecognized star groups, including 16 missed alarm for the small ε, 16 are interfered by binary stars or bad pixels, and 2 contained star which are not in the UCAC4 catalog, one of the star group is interfered by binary stars and stars that are not in the catalog simultaneously. In Figure 3, a star group is incorrectly identified, the main reason is that the magnitude difference between the identified reference star and the correct one is less than 0.2mag. Therefore, it is impossible to eliminate this wrong recognition result according to the magnitude conditions.

Obviously, the success rate of our algorithm is higher than that of the four comparative algorithms, and it can accurately identify the neighboring stars while identifying the reference star. Meanwhile, when the image is mirrored and tilted, our algorithm can still correctly identify stars, while the four comparative algorithms cannot.

VII. CONCLUSION

In this paper, a novel star-ID method based on image normalization technique and the Zernike moment is employed to solve the star-ID problem when optical center coordinates, image rotation angle, focal length of optical system and image sensor's pixel size contain errors or even missing. Experiment results show that our algorithm can accurately identify stars under the prior values. Meanwhile, it can guarantee a high success rate under the condition that the first four parameters in Table 1 are completely missing, and can deal with the interference of pointing error of the ground-based telescope, mirrored star image, tilted image sensor and distortion of the optical system to some extent with strong robustness.

There are still some shortcomings in the algorithm. For example, the correct identification rate is close to zero when a star group contains the star which is not recorded in the catalog. In addition, the algorithm is more time consuming than traditional ones due to the need to traverse the combination of all neighboring stars.

In our future work, we hope to further optimize the speed and adaptability of the algorithm, test our algorithm on more data, and explore some applications of the algorithm on space-based platform.

ACKNOWLEDGMENT

The authors would like to thank the reviewers for their valuable comments and suggestions. They would also like to thank software routines from the IAU SOFA, its work provides them with reliable intermediate data.

REFERENCES

[1] C. Liebe, "Star trackers for attitude determination," *IEEE Aerosp. Electron. Syst. Mag.*, vol. 10, no. 6, pp. 10–16, Jun. 1995.
[2] B. Quine and H. F. Durrant-Whyte, "Rapid star-pattern identification," *Proc. SPIE*, vol. 2739, pp. 351–360, Jun. 1996.
[3] C. Padgett and K. Kreutz-Delgado, "A grid algorithm for autonomous star identification," *IEEE Trans. Aerosp. Electron. Syst.*, vol. 33, no. 1, pp. 202–213, Jan. 1997.
[4] J. Yang, G. Zhang, and J. Jiang, "A star identification algorithm for un-calibrated star sensor cameras," *Opt. Tech.*, vol. 34, pp. 26–32, Aug. 2008.
[5] G. Zhang, X. Wei, and J. Jiang, "Full-sky autonomous star identification based on radial and cyclic features of star pattern," *Image Vis. Comput.*, vol. 26, no. 7, pp. 891–897, Jul. 2008.
[6] J. Li, X. Wei, and G. Zhang, "Iterative algorithm for autonomous star identification," *IEEE Trans. Aerosp. Electron. Syst.*, vol. 51, no. 1, pp. 536–547, Jan. 2015.
[7] M. Aghaei and H. A. Moghaddam, "Grid star identification improvement using optimization approaches," *IEEE Trans. Aerosp. Electron. Syst.*, vol. 52, no. 5, pp. 2080–2090, Oct. 2016.
[8] F. Ji, J. Jiang, and X. Wei, "Unified redundant patterns for star identification," in *Proc. IEEE Int. Conf. Imag. Syst. Techn. (IST)*, Oct. 2013, pp. 228–233.
[9] X. Wei, D. Wen, Z. Song, J. Xi, W. Zhang, G. Liu, and Z. Li, "A star identification algorithm based on radial and dynamic cyclic features of star pattern," *Adv. Space Res.*, vol. 63, no. 7, pp. 2245–2259, Apr. 2019.
[10] X. Liang, J. Zhou, and W. Ma, "Method of distortion and pointing correction of a ground-based telescope," *Appl. Opt.*, vol. 58, no. 19, p. 5136, Jul. 2019.
[11] B.-S. Liu, C.-K. Liu, and H.-T. Du, *The Measuring Equipment Accuracy Appraisal on the Range*, ed. Beijing, China: National Defensen Industry Press, 2008, pp. 203–207.
[12] A. Rosenfeld and A. C. Kak, *Digital Picture Processing*, ed. New York, NY, USA: Academic, 1982, pp. 113–116.
[13] S.-C. Pei and C.-N. Lin, "Image normalization for pattern recognition," *Image Vis. Comput.*, vol. 13, no. 10, pp. 711–723, Dec. 1995.
[14] D. Shen and H. Ip, "Generalized affine invariant image normalization," *IEEE Trans. Pattern Anal. Mach. Intell.*, vol. 19, no. 5, pp. 431–440, May 1997.
[15] G. Zhang, *Star Identification*, 1st ed, H. Wang Ed. Beijing, China: National Defense Industry Press, 2011, pp. 49–62.
[16] A. Khotanzad and Y. Hong, "Invariant image recognition by Zernike moments," *IEEE Trans. Pattern Anal. Mach. Intell.*, vol. 12, no. 5, pp. 489–497, May 1990.
[17] Y. Zhu, M. Xie, and X. Huang, "Studies on object recognition based on combination of image compacting and Zernike moments," *Microelectron. Comput.*, vol. 20, no. 1, pp. 31–34, 2003.
[18] H.-J. Kim and W.-Y. Kim, "Eye detection in facial images using Zernike moments with SVM," *ETRI J.*, vol. 30, no. 2, pp. 335–337, Apr. 2008.
[19] Y. Bin and P. Jia-Xiong, "Invariance analysis of improved Zernike moments," *J. Opt. A, Pure Appl. Opt.*, vol. 4, no. 6, pp. 606–614, Nov. 2002.

XIAOBO LIANG received the bachelor's degree from Sichuan University (SCU), in 2013, and the master's degree from the University of Chinese Academy of Sciences (UCAS), in 2017. His research interests include error correction of large telescope, astronomical orientation, and astronomical positioning.

WENLI MA received the degree from the University of Electronic Science and Technology. He is a Research Fellow and a Doctoral Supervisor with the Institute of Optics and Electronics (IOE), Chinese Academy of Sciences (CAS), China. His research interests include photoelectric detection, precision machinery, and large photoelectric telescope.

JIN ZHOU received the degree from the Institute of Optics and Electronics (IOE), Chinese Academy of Sciences (CAS), China. He has engaged many years on the research of target tracking and recognition, imaging control, target simulation, and intelligent image processing.

SIJIE KONG received the degree from the University of Chinese Academy of Sciences (UCAS). She is mainly engaged in the research of image processing and space debris detection.